

THE EFFECT OF MATRIX PLASTICITY AND DUPLICATE CUTS ON STRESS DISTRIBUTION IN SHORT AND LONG FIBERS OF A HYBRID COMPOSITE LAMINA (PERFECT BOND MODEL)*

M. SHISHEHSAZ

Dept. of Mechanical Eng., Shahid Chamran University, Ahvaz, I. R. of Iran
Email: Shishesaz@yahoo.com

Abstract– Stress distribution in short and long fibers and their surrounding matrix bays of a finite width hybrid composite lamina is examined. The lamina is subjected to a tensile load of magnitude "P" at infinity, while its matrix is assumed to take only shear (shear-lag theory). The bay adjacent to the first intact filament is allowed to experience a plastic zone of size 2α , due to excessive shear load owned by cracks formed by double cuts along each filament. The plastic zone is assumed to behave as elastic–perfectly plastic. The short fibers are simulated by assuming two successive breaks along each filament. The effect of the plastic zone on short fiber load bearing capability, as well as stress concentration in the first intact filament is fully investigated. The effect of hybridization, in the presence of the plastic zone, is also examined on short fiber load bearing behavior.

Keywords– Hybrid, short fiber, plastic zone, elastic-perfectly plastic, stress concentration, shear-lag

1. INTRODUCTION

Due to the low cost and high strength of composite materials, specific attention has been paid to their usage. In order to reach the required mechanical property, one may use composites in a variety of ways, namely in the form of hybrids. By definition, a hybrid composite is one which is composed of more than one filament. This is due to a need for any improvement in a deficiency present in a single type fiber composite. According to the geometric arrangement of fibers, one can categorize the unidirectional hybrid composites into two groups, that is, the interply and intraply (intermingled) hybrids. In the former case, the composite is composed of discrete layers of one fiber only (i.e. a composite tube with graphite inner layers and a glass–epoxy outer layer). The latter group corresponds to the case wherein the fibers are combined in a regular fashion in each ply of the composite. The stress distribution in intraply hybrid composites is the focus of this research. In general, the use of the second type fiber could be to improve the weight of the overall structure, its mechanical property, a reduction in the cost of production and so on. Since the presence of the second type fiber complicates the stress distribution within the material, knowledge of this behavior will enable one to use these materials efficiently. To understand this behavior, the material has to be modeled properly. One of the models available is based on the shear lag theory, where in all fibers are assumed to take the axial load and the matrix sustains only shear. The load transfer mechanism from any broken fiber to the adjacent filament is through shear stress in the matrix. It is shown that [1-3] the shear-lag model gives relatively accurate results on normal stresses developed in composites with a low extensional stiffness in the matrix. Some authors have applied numerical methods to compare the results of the shear-lag theory with those of the finite element method [4-5]. The effect of inter-fiber

*Received by the editors May 15, 2004; final revised form April 26, 2006.

spacing and matrix crack on the stress concentration factor has also been examined by Sirivedin *et al.* [6]. The effect of fiber cross sectional shape on mechanical behavior was further discussed by Bond *et al.* [7].

Oval openings and the way to design for stress reduction due to their presence is discussed [8-9]. Several authors have also studied the stress distribution and fracture behavior of hybrid composites [10-13]. Stress-strain behavior in the initial stage of short fiber reinforced metal matrix composites was studied by Ding and his co-authors [14]. In [15], tensile properties of short glass fiber and short carbon fiber reinforced composites were studied to determine the effect of fiber volume fraction and its length on tensile properties of the overall material.

Most of the research on composites with matrix plasticity has focused on materials with single-type filament [16-18]. Due to the complexity of stress distribution in short fiber composites, and even more, hybrid composites, and stress distribution in this field have many unresolved questions which have yet to be answered. In this paper, an effort is made to understand this behavior in more detail.

2. DERIVATION OF FORMULAS

To obtain the necessary relations, a finite width composite lamina with $N=2q+1$ fibers is considered (Fig. 1). It is assumed that all the fibers are aligned in parallel, and the spacing between them, namely "h", is equal to the fiber's diameter "d". Furthermore, it is assumed that all fibers will only take extensional load, and the matrix sustains only shear. This is a good assumption for most composites with a phenolic resin or weakness in tension.

The high modulus fibers (HM), as well as the low modulus fibers (LM), are assumed to have the same diameter and act as linear elastic materials up to the point of fracture. Two successive breaks are considered along each filament to simulate a short fiber. A perfect bond is assumed to exist between the fibers and the matrix, while each bay bonding the crack tip (formed by the breaks) is experiencing a plastic zone of size 2α , due to the presence of excessive shear stress. The stress in this zone is assumed to behave as elastic-perfectly plastic. The lamina is subjected to a tensile load of magnitude P, applied at infinity. Due to symmetry, only the right portion of the lamina is considered (Fig. 2).

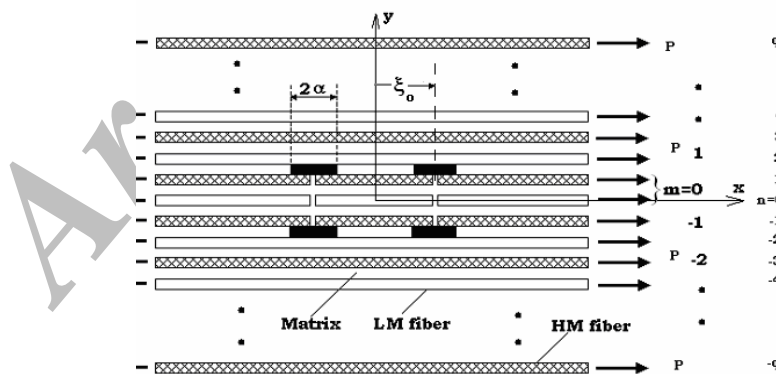


Fig. 1. Fiber arrangement in a hybrid lamina with double cuts

To obtain the field equations, the right portion is divided into two regions. Each region deals with two subregions. Subregions 1.1 and 2.1 deal with zones where the matrix bays bonding the crack tip have experienced yielding. Equilibrium equations in each region are then written by considering a volume element containing two successive fibers (one HM and one LM fiber), and their surrounded matrix bay as shown in Fig. 3. Application of the force equilibrium equation along x on the m^{th} volume element in the elastic zone of region 2 reveals that

$$E_f A_f \frac{d^2 u_m^{(2)}}{dx^2} + \frac{Gh}{d} (u_m^{*(2)} - 2u_m^{(2)} + u_{m-1}^{*(2)}) = 0 \quad (1)$$

$$E_f^* A_f^* \frac{d^2 u_m^{*(2)}}{dx^2} + \frac{Gh}{d} (u_m^{(2)} - 2u_m^{*(2)} + u_{m-1}^{(2)}) = 0 \quad (2)$$

Where for the elastic zone of region one we may write

$$E_f A_f \frac{d^2 u_m^{(1)}}{dx^2} + \frac{Gh}{d} (u_m^{*(1)} - 2u_m^{(1)} + u_{m-1}^{*(1)}) = 0 \quad (3)$$

$$E_f^* A_f^* \frac{d^2 u_m^{*(1)}}{dx^2} + \frac{Gh}{d} (u_{m+1}^{(1)} - 2u_m^{*(1)} + u_m^{(1)}) = 0 \quad (4)$$

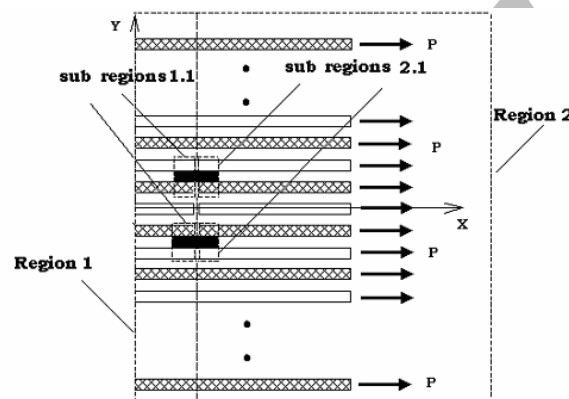


Fig. 2. Fiber arrangement for the right hand portion of the lamina

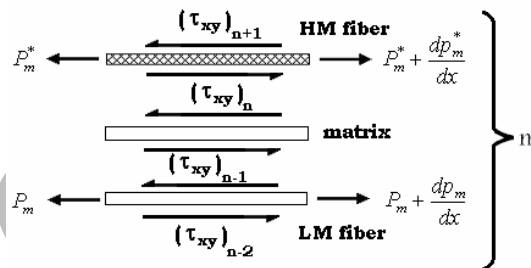


Fig. 3. Force equilibrium on the m^{th} volume element

In the above equations, superscripts (1) and (2) are used for regions one and two respectively, while the asterisk is used to distinguish those properties associated with LM fibers. Assuming the lamina ends in HM fibers on the edge, the equilibrium equations for the edge fibers in region two reduce into:

$$E_f A_f \frac{d^2 u_n^{(2)}}{dx^2} + \frac{Gh}{d} (u_{n-1}^{*(2)} - u_n^{(2)}) = 0 \quad n = q \quad (5)$$

$$E_f A_f \frac{d^2 u_n^{(2)}}{dx^2} + \frac{Gh}{d} (u_{n+1}^{*(2)} - u_n^{(2)}) = 0 \quad n = -q \quad (6)$$

And for region one

$$E_f A_f \frac{d^2 u_n^{(1)}}{dx^2} + \frac{Gh}{d} (u_{n-1}^{*(1)} - u_n^{(1)}) = 0 \quad n = q \quad (7)$$

$$E_f A_f \frac{d^2 u_n^{(1)}}{dx^2} + \frac{Gh}{d} (u_{n+1}^{*(1)} - u_n^{(1)}) = 0 \quad n = -q \quad (8)$$

For simplicity, equilibrium Eqs. (1) through (8) are written in a non-dimensional form as follows.

$$\frac{d^2 U_m^{(2)}}{d\xi^2} + (U_m^{*(2)} - 2U_m^{(2)} + U_{m-1}^{*(2)}) = 0 \quad (9)$$

$$R \frac{d^2 U_m^{*(2)}}{d\xi^2} + (U_m^{(2)} - 2U_m^{*(2)} + U_{m-1}^{(2)}) = 0 \quad (10)$$

$$\frac{d^2 U_m^{(1)}}{d\xi^2} + (U_m^{*(1)} - 2U_m^{(1)} + U_{m-1}^{*(1)}) = 0 \quad (11)$$

$$R \frac{d^2 U_m^{*(1)}}{d\xi^2} + (U_m^{(1)} - 2U_m^{*(1)} + U_{m-1}^{(1)}) = 0 \quad (12)$$

$$\frac{d^2 U_n^{(2)}}{d\xi^2} + (U_{n-1}^{*(2)} - U_n^{*(2)}) = 0 \quad n = q \quad (13)$$

$$\frac{d^2 U_n^{(2)}}{d\xi^2} + (U_{n+1}^{*(2)} - U_n^{(2)}) = 0 \quad n = -q \quad (14)$$

$$\frac{d^2 U_n^{(1)}}{d\xi^2} + (U_{n-1}^{*(1)} - U_n^{(1)}) = 0 \quad n = q \quad (15)$$

$$\frac{d^2 U_n^{(1)}}{d\xi^2} + (U_{n+1}^{*(1)} - U_n^{(1)}) = 0 \quad n = -q \quad (16)$$

Similar expressions to those of (13) through (16) may be written if the edges end in an LM fiber. Allow "T" to be the non-dimensional yield stress in the matrix and \bar{U} to correspond to the non-dimensional displacement associated with the portion of those fibers adjacent to the yield zones (sub regions 1.1 and 2.1), then for those fibers in sub regions 1.1 and bonding the plastic zone, the equilibrium equations become:

$$R \frac{d^2 \bar{U}_n^{*(1)}}{d\xi^2} + (\bar{U}_{n+1}^{(1)} - \bar{U}_n^{*(1)}) - T = 0 \quad n = (r+1)/2 \quad (17)$$

$$\frac{d^2 \bar{U}_n^{(1)}}{d\xi^2} + (\bar{U}_{n-1}^{*(1)} - \bar{U}_n^{(1)}) + T = 0 \quad n = (r-1)/2 \quad (18)$$

$$\frac{d^2 \bar{U}_n^{(1)}}{d\xi^2} + (\bar{U}_{n+1}^{*(1)} - \bar{U}_n^{(1)}) - T = 0 \quad n = -(r-1)/2 \quad (19)$$

$$R \frac{d^2 \bar{U}_n^{*(1)}}{d\xi^2} + (\bar{U}_{n+1}^{(1)} - \bar{U}_n^{*(1)}) - T = 0 \quad n = -(r+1)/2 \quad (20)$$

where it has been assumed that an LM fiber bonds the crack tip and the breaks are symmetric with respect to $n = 0$ fiber.

In addition, for sub-regions 2.1, the equilibrium equations for those fibers bonding the plastic zone reduce into:

$$R \frac{d^2 \bar{U}_n^{*(2)}}{d\xi^2} + (\bar{U}_{n+1}^{(2)} - \bar{U}_n^{*(2)}) - T = 0 \quad n = (r+1)/2 \quad (21)$$

$$\frac{d^2 \bar{U}_n^{(2)}}{d\xi^2} + (\bar{U}_{n-1}^{*(2)} - \bar{U}_n^{(2)}) + T = 0 \quad n = (r-1)/2 \quad (22)$$

$$\frac{d^2 \bar{U}_n^{(2)}}{d\xi^2} + (\bar{U}_{n+1}^{*(2)} - \bar{U}_n^{(2)}) - T = 0 \quad n = -(r-1)/2 \quad (23)$$

$$R \frac{d^2 \bar{U}_n^{*(2)}}{d\xi^2} + (\bar{U}_{n+1}^{(2)} - \bar{U}_n^{*(2)}) - T = 0 \quad n = -(r+1)/2 \quad (24)$$

Similar expressions may be written if an HM fiber bonds the crack tip.

3. DISPLACEMENT AND LOAD DISTRIBUTION FIELDS

a) Elastic regions

For elastic regions one and two, Eqs. (2.9) through (2.16) may be written in a matrix notation as:

$$\mathbf{I}_1 \mathbf{U}''^{(1)} - \mathbf{I}_2 \mathbf{U}^{(1)} = 0 \quad (25)$$

$$\mathbf{I}_1 \mathbf{U}''^{(2)} - \mathbf{I}_2 \mathbf{U}^{(2)} = 0 \quad (26)$$

Where \mathbf{I}_1 and \mathbf{I}_2 are coefficient matrices and \mathbf{U}'' corresponds to the second derivative of \mathbf{U} with respect to ξ . Hence, the solution to the differential-difference Eqs. (25) and (26), in elastic zones of the two regions may be written as follows.

1. Region one: In this region, the solution to Eq. (25) may be written in terms of eigen values λ_i and eigen vectors $\mathbf{R}^{(i)}$ as;

$$U_n^{(1)} = \xi + \sum_{i=1}^{2q+1} (A_i R_{(q-n+1)}^{(i)} e^{\lambda_i \xi} + B_i R_{(q-n+1)}^{(i)} e^{-\lambda_i \xi}) \quad (27)$$

$$P_n^{(1)} = 1 + \sum_{i=1}^{2q+1} (A_i \lambda_i e^{\lambda_i \xi} - B_i \lambda_i e^{-\lambda_i \xi}) R_{(q-n+1)}^{(i)} \quad (\text{for HM fibers}) \quad (28)$$

$$P_n^{*(1)} = R \left\{ 1 + \sum_{i=1}^{2q+1} (A_i \lambda_i e^{\lambda_i \xi} - B_i \lambda_i e^{-\lambda_i \xi}) R_{(q-n+1)}^{(i)} \right\} \quad (\text{for LM fibers}) \quad (29)$$

This excludes the solution to the portion of those two fibers in contact with the plastic zone and bonding each crack tip in subregions 1.1. In the equations above, $R_{(q-n+1)}^{(i)}$ is a value associated with the $(q-n+1)^{\text{th}}$ row of the i^{th} eigen vector.

2. Region two: In this region, solving Eq. (2), similar expressions to those of (27)-(29) may be written as:

$$U_n^{(2)} = \xi + \sum_{i=1}^{2q+1} (D_i R_{(q-n+1)}^{(i)}) e^{-\lambda_i \xi} \quad (30)$$

$$P_n^{(2)} = 1 + \sum_{i=1}^{2q+1} (-D_i \lambda_i e^{-\lambda_i \xi}) R_{(q-n+1)}^{(i)} \quad (\text{for HM fibers}) \quad (31)$$

$$P_n^{*(2)} = R \left\{ 1 + \sum_{i=1}^{2q+1} (-D_i \lambda_i e^{-\lambda_i \xi}) R_{(q-n+1)}^{(i)} \right\} \quad (\text{for LM fibers}) \quad (32)$$

This excludes the solution to the portion of those two fibers in contact with the plastic zone and bonding each crack tip in subregions 2.1. In Eqs. (30)-(32), positive values of λ_i are discarded due to the bond ness conditions below:

$$\begin{cases} P_n = 1 \\ P_n^* = R \end{cases} \quad \text{as } \xi \rightarrow \infty \quad (33)$$

in the above equations. A_i , B_i , and D_i , are constants yet to be defined from boundary conditions.

b) Plastic regions

1. Subregions 1.1: For those fibers in the vicinity of the yielded zone, the homogeneous solution of the displacement fields (Eqs. (18)-(21)) may be written as:

$$(\bar{U}_n^{*(1)})_H = P_1 e^{\frac{-\xi}{\sqrt{R}}} + P_2 e^{\frac{\xi}{\sqrt{R}}} \quad n = (r+1)/2 \quad (34)$$

$$(\bar{U}_n^{(1)})_H = Q_1 e^{-\xi} + Q_2 e^{\xi} \quad n = (r-1)/2 \quad (35)$$

$$(\bar{U}_n^{(1)})_H = S_1 e^{-\xi} + S_2 e^{\xi} \quad n = -(r-1)/2 \quad (36)$$

$$(\bar{U}_n^{*(1)})_H = R_1 e^{\frac{-\xi}{\sqrt{R}}} + R_2 e^{\frac{\xi}{\sqrt{R}}} \quad n = -(r+1)/2 \quad (37)$$

Where P_1 , P_2 , Q_1 , Q_2 ,, R_1 , and R_2 are constants yet to be defined. The complete displacement field for a typical LM fiber in this region is then:

$$\bar{U}_n^{*(1)} = (\bar{U}_n^{*(1)})_H + (\bar{U}_n^{*(1)})_P \quad (38)$$

Where $(\bar{U}_n^{*(1)})_P$ is the particular solution for a portion of a typical LM fiber in sub-region 1.1, bonding the crack tip. One can show that the expression for $(\bar{U}_n^{*(1)})_P$ may be written as:

$$(\bar{U}_n^{*(1)})_P = T + \xi + \sum_{i=1}^{2q-1} \frac{C_i R_{(q-n+2)}^{(i)}}{R \lambda_i^2 - 1} e^{\lambda_i \xi} - \sum_{i=1}^{2q-1} \frac{D_i R_{(q-n+2)}^{(i)}}{R \lambda_i^2 - 1} e^{-\lambda_i \xi} \quad (39)$$

where D_i are the same unknown constants given previously in Eq. (30). A similar procedure may be adapted to obtain an expression for an HM fiber, when bonding the crack tip.

2. Subregions 2.1: It may be shown that the displacement fields for those fibers bonding the yielded zone of sub-region 2.1 may be written as:

$$\bar{U}_n^{*(2)} = P_1' e^{-\frac{\xi}{\sqrt{R}}} + P_2' e^{\frac{\xi}{\sqrt{R}}} + T + \xi - \sum_{i=1}^{2q-1} \frac{A_i R_{(q-n+2)}^{(i)}}{R\lambda_i^2 - 1} e^{-\lambda_i \xi_i} \quad n = (r+1)/2 \quad (40)$$

$$\bar{U}_n^{(2)} = Q_1' e^{-\xi} + Q_2' e^{\xi} + T + \xi - \sum_{i=1}^{2q-1} \frac{A_i R_{(q-n-1)}^{(i)}}{\lambda_i^2 - 1} e^{-\lambda_i \xi_i} \quad n = (r-1)/2 \quad (41)$$

$$\bar{U}_n^{(2)} = S_1' e^{-\xi} + S_2' e^{\xi} + T + \xi - \sum_{i=1}^{2q-1} \frac{A_i R_{(q-n-1)}^{(i)}}{\lambda_i^2 - 1} e^{-\lambda_i \xi_i} \quad n = -(r-1)/2 \quad (42)$$

$$\bar{U}_n^{*(2)} = R_1' e^{-\frac{\xi}{\sqrt{R}}} + R_2' e^{\frac{\xi}{\sqrt{R}}} + T + \xi - \sum_{i=1}^{2q-1} \frac{A_i R_{(q-n+2)}^{(i)}}{R\lambda_i^2 - 1} e^{-\lambda_i \xi_i} \quad n = -(r+1)/2 \quad (43)$$

Where A_i are those constants expressed in Eq. (27).

Knowing the displacement fields above, the load in each fiber is obtained using the following relation:

$$P_n = \frac{dU_n}{d\xi} \quad (44)$$

4. BOUNDARY CONDITIONS AND CONTINUITY EQUATIONS

To solve for the constants introduced in displacement fields, defining $\xi_1 + \alpha = \xi_0$, the following boundary conditions and continuity equations may be introduced.

$$U_n^{(1)}(0) = 0 \quad -2q-1 \leq n \leq 2q+1 \quad (45)$$

$$U_n^{*(1)}(0) = 0 \quad -2q-1 \leq n \leq 2q+1 \quad (46)$$

$$\begin{aligned} \text{either } U_n^{(1)}(\xi_1) &= \bar{U}_n^{(1)}(\xi_1) & n &= (r+1)/2, -(r+1)/2 \\ P_n^{(1)}(\xi_1) &= \bar{P}_n^{(1)}(\xi_1) & n &= (r+1)/2, -(r+1)/2 \end{aligned} \quad (47)$$

$$\begin{aligned} \text{or } U_n^{*(1)}(\xi_1) &= \bar{U}_n^{*(1)}(\xi_1) & n &= (r+1)/2, -(r+1)/2 \\ P_n^{*(1)}(\xi_1) &= \bar{P}_n^{*(1)}(\xi_1) & n &= (r+1)/2, -(r+1)/2 \end{aligned}$$

$$\begin{aligned} \text{either } U_n^{*(1)}(\xi_1) &= \bar{U}_n^{*(1)}(\xi_1) & n &= (r-1)/2, -(r-1)/2 \\ P_n^{*(1)}(\xi_1) &= \bar{P}_n^{*(1)}(\xi_1) & n &= (r-1)/2, -(r-1)/2 \end{aligned} \quad (48)$$

$$\begin{aligned} \text{or } U_n^{(1)}(\xi_1) &= \bar{U}_n^{(1)}(\xi_1) & n &= (r-1)/2, -(r-1)/2 \\ P_n^{(1)}(\xi_1) &= \bar{P}_n^{(1)}(\xi_1) & n &= (r-1)/2, -(r-1)/2 \end{aligned}$$

$$U_n^{(1)}(\xi_1 + \alpha) = U_n^{(2)}(\xi_1 + \alpha) \quad \begin{aligned} (r+1)/2 < n \leq 2q+1 \\ |-(r+1)/2| < |n| \leq |-2q-1| \end{aligned} \quad (49)$$

$$U_n^{*(1)}(\xi_1 + \alpha) = U_n^{*(2)}(\xi_1 + \alpha) \quad \begin{aligned} (r+1)/2 < n \leq 2q+1 \\ |-(r+1)/2| < |n| \leq |-2q-1| \end{aligned} \quad (50)$$

$$P_n^{(1)}(\xi_1 + \alpha) = P_n^{(2)}(\xi_1 + \alpha) \quad \begin{aligned} (r+1)/2 < n \leq 2q+1 \\ |-(r+1)/2| < |n| \leq |-2q-1| \end{aligned} \quad (51)$$

$$P_n^{*(1)}(\xi_1 + \alpha) = P_n^{*(2)}(\xi_1 + \alpha) \quad \begin{array}{l} (r+1)/2 < n \leq 2q+1 \\ |-(r+1)/2| < |n| \leq |-2q-1| \end{array} \quad (52)$$

$$P_n^{(1)}(\xi_1 + \alpha) = 0 \quad -(r-3)/2 \leq n \leq (r-3)/2 \quad (53)$$

$$P_n^{*(1)}(\xi_1 + \alpha) = 0 \quad -(r-3)/2 \leq n \leq (r-3)/2 \quad (54)$$

$$P_n^{(2)}(\xi_1 + \alpha) = 0 \quad -(r-3)/2 \leq n \leq (r-3)/2 \quad (55)$$

$$P_n^{*(2)}(\xi_1 + \alpha) = 0 \quad -(r-3)/2 \leq n \leq (r-3)/2 \quad (56)$$

$$\bar{U}_n^{(1)}(\xi_1 + \alpha) = \bar{U}_n^{(2)}(\xi_1 + \alpha) \quad \begin{array}{l} n = (r+1)/2 \\ n = -(r+1)/2 \end{array} \quad (57)$$

$$\bar{P}_n^{(1)}(\xi_1 + \alpha) = \bar{P}_n^{(2)}(\xi_1 + \alpha) \quad \begin{array}{l} n = (r+1)/2 \\ n = -(r+1)/2 \end{array} \quad (58)$$

or

$$\bar{U}_n^{*(1)}(\xi_1 + \alpha) = \bar{U}_n^{*(2)}(\xi_1 + \alpha) \quad \begin{array}{l} n = (r+1)/2 \\ n = -(r-1)/2 \end{array} \quad (59)$$

$$\bar{P}_n^{*(1)}(\xi_1 + \alpha) = \bar{P}_n^{*(2)}(\xi_1 + \alpha) \quad \begin{array}{l} n = (r+1)/2 \\ n = -(r+1)/2 \end{array} \quad (60)$$

$$\bar{P}_n^{(1)}(\xi_1 + \alpha) = 0 \quad \begin{array}{l} n = (r-1)/2 \\ n = -(r-1)/2 \end{array} \quad (61)$$

$$\bar{P}_n^{(2)}(\xi_1 + \alpha) = 0 \quad \begin{array}{l} n = (r-1)/2 \\ n = -(r-1)/2 \end{array} \quad (62)$$

or

$$\bar{P}_n^{*(1)}(\xi_1 + \alpha) = 0 \quad \begin{array}{l} n = (r-1)/2 \\ n = -(r-1)/2 \end{array} \quad (63)$$

$$\bar{P}_n^{*(2)}(\xi_1 + \alpha) = 0 \quad \begin{array}{l} n = (r-1)/2 \\ n = -(r-1)/2 \end{array} \quad (64)$$

$$U_n^{(2)}(\xi_1 + \alpha) = \bar{U}_n^{(2)}(\xi_1 + \alpha) \quad \begin{array}{l} n = (r-1)/2, (r+1)/2 \\ n = -(r-1)/2, -(r-1)/2 \end{array} \quad (65)$$

$$P_n^{(2)}(\xi_1 + \alpha) = \bar{P}_n^{(2)}(\xi_1 + \alpha) \quad \begin{array}{l} n = (r-1)/2, (r+1)/2 \\ n = -(r-1)/2, -(r+1)/2 \end{array} \quad (66)$$

or

$$U_n^{*(2)}(\xi_1 + \alpha) = \bar{U}_n^{*(2)}(\xi_1 + \alpha) \quad \begin{array}{l} n = (r-1)/2, (r+1)/2 \\ n = -(r-1)/2, -(r-1)/2 \end{array} \quad (67)$$

$$P_n^{*(2)}(\xi_1 + \alpha) = \bar{P}_n^{*(2)}(\xi_1 + \alpha) \quad \begin{array}{l} n = (r-1)/2, (r+1)/2 \\ n = -(r-1)/2, -(r-1)/2 \end{array} \quad (68)$$

The non-dimensional yield stress may also be expressed using one of the following relations:

$$T^{(1)} = \bar{U}_n^{(1)}(\xi_1) - U_{n+1}^{*(1)}(\xi_1) \quad n = (r-1)/2, -(r-1)/2 \quad (69)$$

$$T^{(2)} = \bar{U}_n^{(2)}(\xi_1 + 2\alpha) - U_{n+1}^{*(2)}(\xi_1 + 2\alpha) \quad n = (r-1)/2, -(r-1)/2 \quad (70)$$

$$T^{*(1)} = \bar{U}_n^{*(1)}(\xi_1) - U_{n+1}^{(1)}(\xi_1) \quad n = (r-1)/2, -(r-1)/2 \quad (71)$$

$$T^{*(2)} = \bar{U}_n^{*(2)}(\xi_1 + 2\alpha) - U_{n+1}^{(2)}(\xi_1 + 2\alpha) \quad n = (r-1)/2, -(r-1)/2 \quad (72)$$

One can use the above boundary conditions and continuity equations to solve the 3n-20 unknowns present in equilibrium equations.

5. MECHANICAL PROPERTIES OF THE SELECTED ELEMENTS

In order to investigate the effect of plastic zone size on stress variation within the lamina, using [19], the following values were selected for fiber and matrix properties.

Table 1. Mechanical properties of selected materials forming the hybrid lamina

Element	Modulus of elasticity
Epoxy matrix	2.8-4.2 Gpa
Graphite fiber	248 Gpa
Glass fiber	
S-Glass	85.5 Gpa
E-Glass	72.4 Gpa

6. RESULTS AND DISCUSSION

In Figs. 4-9, it is assumed that the breaks grow symmetric with respect to lamina width. The effect of hybridization on stress concentration in LM fibers and in the presence of a plastic zone is shown in Fig. 4 for $r=5$ and $\xi_0=2$. In a hybridized composite with no plastic zone, the stress concentration factor in an LM fiber is always higher than that associated with a single type fibrous composite subjected to a similar loading condition. This behavior is also observed for small plastic zone sizes bonding the crack tip. As α is increased, the effect of hybridization on K_r appears to be decreased. This effect seems to be considerable for all values of R ranging from $0 < R \leq 1$. For example, at $\alpha = 0$, once the lamina is hybridized to $R=0.2$, the stress concentration in the first intact filament has increased by 69.4%, while in the presence of a plastic zone of size $\alpha=0.4$, the increase is only 13.4%. For $R=0.33$, a typical value of glass-boron-epoxy composite, hybridization causes a 40% increase in K_r at $\alpha=0$, and a 6.1% decrease at $\alpha = 0.4$. Both of these changes are for $r=5$ ($2a/w \approx 0.27$).

As shown in Fig. 5, opposite results are obtained when an HM fiber bonds the crack tip. This is due to the nature of complex stress distribution and displacement fields in hybrid composites subjected to an internal discontinuity in the form of a crack [12, 20, 21]. In the presence of a no plastic zone, an HM fiber always takes fewer loads compared to that of a non-hybrid composite, provided the loading condition remains intact. The same behavior is also observed in the presence of a very small plastic zone at the crack tip. As the size of the plastic zone is increased, the values of the stress concentration factor in HM fibers reach and go beyond those associated with $R=1$. This effect seems to be present for all values of R ranging

from $0 < R \leq 1$. The percentage decrease in K_r between the two cases of $R=1$ and 0.2 appears to be 18.5% at $\alpha = 0$ and 12.8 % at $\alpha=0.4$. For $R=0.33$, hybridization causes a 15% decrease in K_r at $\alpha=0$, while the reduction is only 7.7% at $\alpha=0.4$. For $\alpha = 0.4$, the percentage increase in K_r becomes 12% as R is decreased from 1 to 0.8.

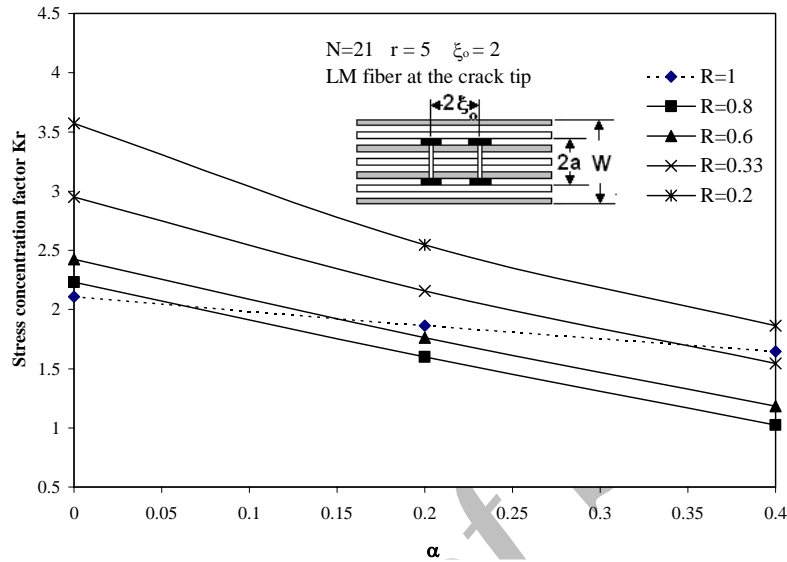


Fig. 4. The effect of plastic zone growth on stress concentration within the lamina for a specific crack size

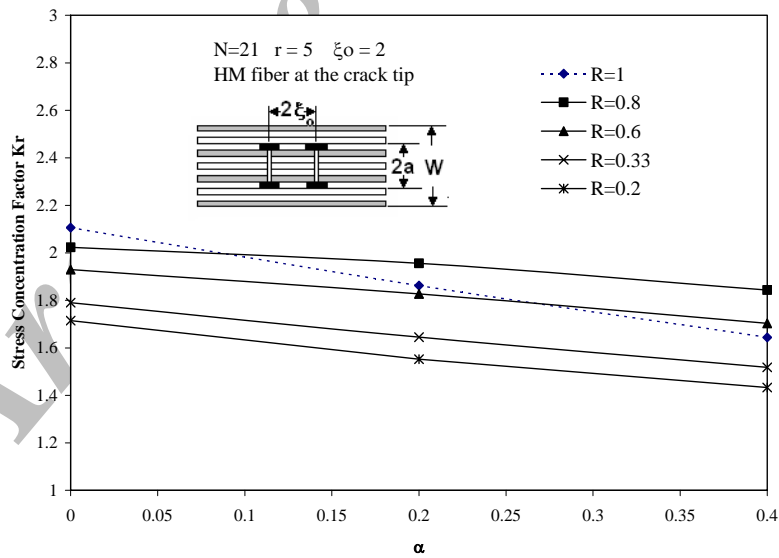


Fig. 5. The effect of plastic zone growth on stress concentration in the first HM filament bonding the crack tip

In both Figs. 6 and 7, the percentage decrease (or increase) in $(P_s)_{max}$ corresponds to a change in R from 1 (single type or non-hybrid fibrous lamina) to 0.33 (hybrid glass-graphite –epoxy composite).

According to Fig. 6, smaller HM short fibers are more sensitive to a plastic zone growth. The percentage reduction in $(P_s)_{max}$, for $\xi_0=2$, is 3.8% at $\alpha/\xi_0 = 0$ and 16.5% at $\alpha=0.8$ (or $\alpha/\xi_0 = 0.4$). A similar result for $\xi_0 = 4$ and at $\alpha/\xi_0 = 0$ is 1%, while for a plastic zone the size of $\alpha=0.8$ ($\alpha/\xi_0 = 0.2$), the percentage decrease appears to be 2.6%. For $\xi_0=4$ and at $\alpha/\xi_0=0.4$ the percentage decrease is 4.1%. The

percentage increase in $(P_s)_{max}$ for all values of ξ_o seems to increase, as the size of the plastic zone is increased.

Figure 7, on the other hand, shows the percentage increase in K_r for an LM short fiber adjacent to the crack tip. Here, the same values of R and ξ_o , are used for further comparison. As it appears, with an increase in α , the percentage increase in $(P_s)_{max}$ appears to be nearly a constant for larger values of ξ_o (3 or 4). The percentage increase in $(P_s)_{max}$ for smaller short fibers, ($\xi_o = 2$), appears to decrease as the size of the plastic zone is increased. For $\xi_o = 2$, the increase in this load is 13.1% at $\alpha/\xi_o = 0$ and 9.8% at $\alpha/\xi_o = 0.4$.

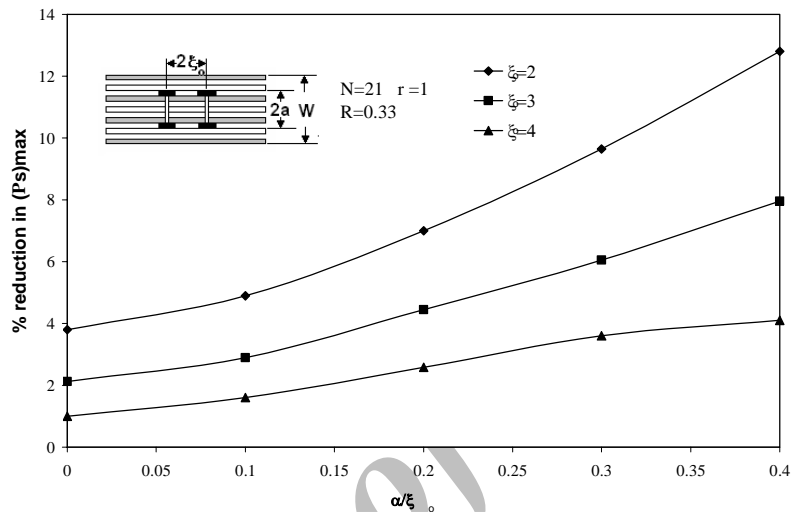


Fig. 6. The effect of matrix plastic zone growth on % reduction in peak normal stress in HM short fiber adjacent to the crack tip

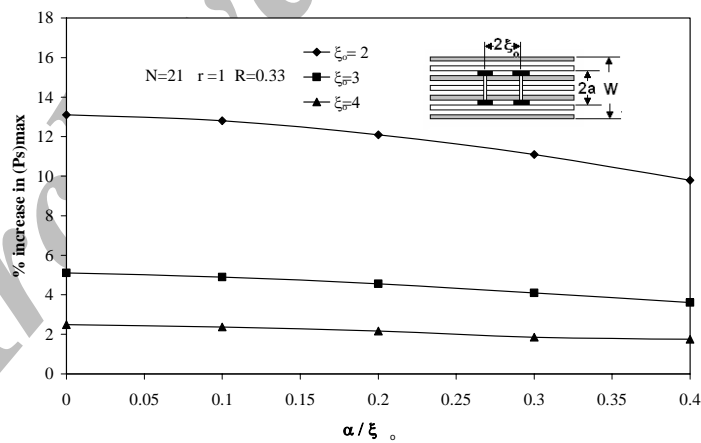


Fig. 7. The effect of matrix plastic zone growth on % reduction in peak normal stress in LM short fiber adjacent to the crack tip

Figure 8 investigates the effect of ξ_o on stress concentration factor K_r in LM fiber bonding the crack tip. Here it is assumed that $R=0.33$, $r=5$, and α ranges from zero to 0.4. Using this figure, one can conclude that for various values of α , an increase in ξ_o greater than 2.5 has almost no effect on a change in K_r . This means that the interaction of the two breaks on each other, and finally on K_r becomes negligible and the results approach those of a single cut along each fiber. The same behavior is also observed when an HM fiber bonds the crack tip, as shown in Fig. 9.

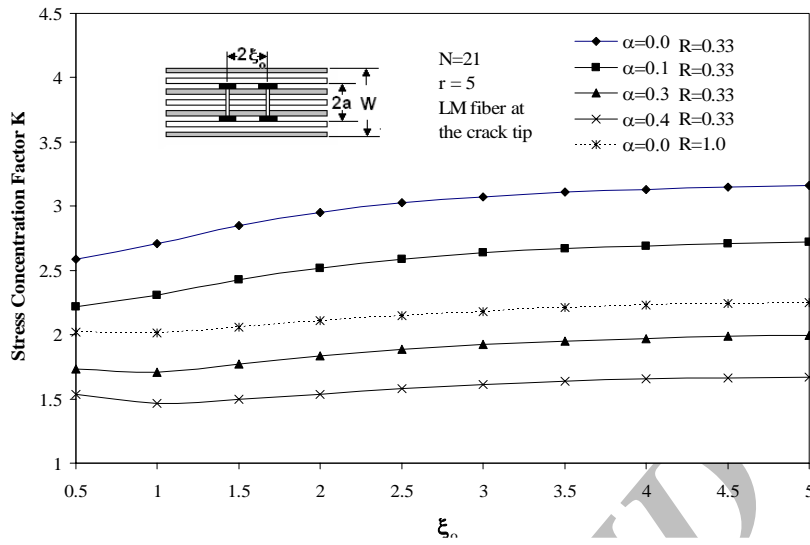


Fig. 8. Variation of stress concentration factor with respect to the length of short fibers

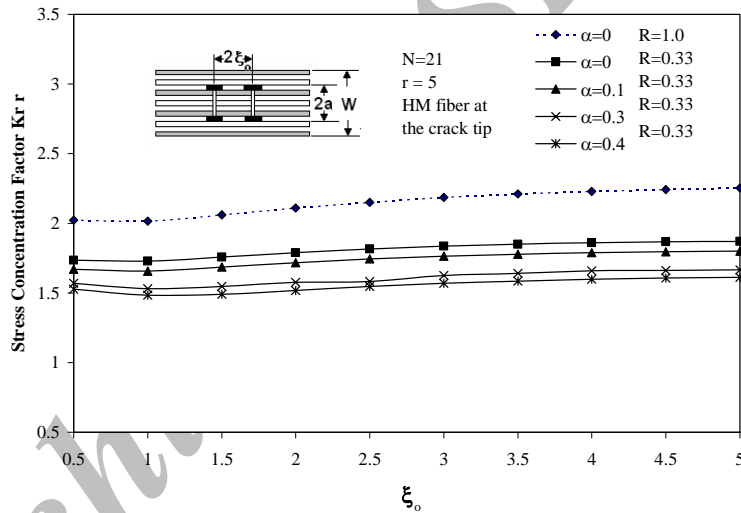


Fig. 9. Variation of stress concentration factor with respect to the length of short fibers

7. CONCLUSIONS

According to the results, one can conclude that in a non-hybrid composite lamina ($R=1$), the presence of the plastic zone on stress reduction in intact filaments becomes more effective as the number of broken fibers grows in size (larger cracks). As the lamina is hybridized, for any value of "R", the growth of the plastic zone appears to lower the value of K_r in both HM and LM fibers. Although in a hybrid composite LM fibers take more load compared to those of $R=1$, the results indicate that for all values of R, as α grows in size, the magnitudes of K_r approach (and even go beyond) those of a non-hybrid composite. A similar behavior is also detected for K_r in HM fibers. In other words, in a hybridized model, the growth of α forces the values of K_r to approach those of a non hybrid composite lamina. It is also recognized that for any value of R and α , the increase in ξ_0 does not appear to have a considerable effect on K_r , provided the distance between any two successive cuts along each filament is more than 5 ($\xi_0=2.5$). The peak load reduction in HM short fibers seems to be more sensitive to α for smaller values of ξ_0 . For LM short fibers, the percentage increase in $(P_s)_{max}$ obeys the same behavior, while its value seems to be almost independent of α for longer short fibers.

NOMENCLATURE

2a	size of the crack
A_f	cross sectional areas of the HM fibers
A_f^*	cross sectional areas of the LM fibers
d	fiber diameter, fiber spacing
E_f, E_f^*	elastic Modulus of the HM and LM fibers, respectively
G	shear modulus of the matrix
h	thickness of the lamina
K_r	stress concentration factor in each fiber
m	volume element containing one HM and one LM fiber
n	filament number
N	total number of fibers ($N=2q+1$)
p	normal Load applied at infinity
P	non-dimensional load in HM Fibers
P^*	non-dimensional load in LM Fibers
2a	size of the crack
A_f	cross sectional areas of the HM fibers
A_f^*	cross sectional areas of the LM fibers
d	fiber diameter, fiber spacing
E_f, E_f^*	elastic Modulus of the HM and LM fibers, respectively
G	shear modulus of the matrix
h	thickness of the lamina
K_r	stress concentration factor in each fiber
m	volume element containing one HM and one LM fiber
n	filament number
N	total number of fibers ($N=2q+1$)
p	normal Load applied at infinity
P	non dimensional load in HM Fibers
P^*	non dimensional load in LM Fibers
$\bar{P}^{(1)}, \bar{P}^{(2)}$	non dimensional loads in a portion of the fibers bonding the yield zone in sub-regions 1.1 and 2.1 respectively
P_s	non-dimensional load in short Fibers
R	extensional stiffness ratio of LM fibers to HM fibers
r	total number of broken fibers
T	non-dimensional yield stress in the matrix
$u^{(1)}$	displacement of fibers in region one
$U^{(1)}$	non dimensional displacement of fibers in region one
$u^{(2)}$	displacement of fibers in region two
$U^{(2)}$	non-dimensional displacement of fibers in region two
$\bar{u}^{(1)}, \bar{U}^{(1)}$	displacement of a portion of the fibers bonding the yield zone (and its non dimensional form) in sub regions 1.1
$\bar{u}^{(2)}, \bar{U}^{(2)}$	displacement of a portion of the fibers bonding the yield zone (and its non-dimensional form) in sub regions 2.1
W	width of the lamina
x,y	coordinate system centered in the middle of the lamina
2 α	non-dimensional size of the plastic zone
λ_i	Eigen value
ξ	non-dimensional coordinate along each filament
2 ξ_0	total length of each short fiber
τ_y	yield stress in the matrix

REFERENCES

1. Hedgepeth, J. M. (1961). Stress concentrations in filamentary structures. NASA-TND 882, may.
2. Rossettos, J. N. & Shishehsaz, M. (1987). Stress concentration in fiber composite sheets including matrix extension. *Journal of Applied Mechanics*, 54.

3. Shishehsaz, M. (2001). The effect of matrix extension on fiber stresses and matrix debonding in a hybrid composite monolayer. *Iranian Journal of Science and Technology, Transaction B*, 25(B2).
4. Reedy, E. D. (1984). Fiber stresses in cracked monolayers: comparison of shear-lag and 3-D finite element predictions. *Journal of Composite Materials*, 18.
5. Xia, Z., Okabe, T. & Curtin, W. A. (2002). Shear-lag versus finite element methods for stress transfer in fiber-reinforced composites. *Journal of Composites Science and Technology*, 62.
6. Sirivedin, S., Fenner, D. N., Nath, R. B. & Galiotis, C. (2003). Effects of inter-fiber spacing and matrix cracks on stress amplification factors in carbon-fiber/epoxy matrix composites. Part I: planar array of fibers", *Journal of Composites, Part A: Applied Science and Manufacturing*, 34.
7. Bond, I., Hucker, M., Weaver, P., Bleay, St. & Haq, S. (2002). Mechanical behavior of circular and triangular glass fibers and their composites. *Journal of Composites Science and Technology*, 62.
8. Allam, M. N. M. & Zenkour, A. M. (2003). Stress concentration factor of a structurally anisotropic composite plate weakened by an oval opening. *Journal of Composite Structures*, 61.
9. Tenchev, R. T., Nygard, M. K. & Echtermeyer, A. (1995). Design procedure for reducing the stress concentration around circular holes in laminated composites. *Journal of Composites*, 26.
10. Fukuda, H. (1983). An advanced theory of strength of hybrid composites. *Journal of Material Science*, 19.
11. Fukuda, H. & Chou, T. W. (1980). Stiffness and strength of hybrid composites. *Proc. Japan -US Conference*, Tokyo.
12. Shishehsaz, M. (1990). Hybridization effect on stress distribution in short fiber composite monolayer of finite width. CSME Mechanical Engineering Forum, Toronto, Canada.
13. Dlouhy, I., Chlup, Z., Boccaccini, D. N., Atiq, S. & Boccaccini, A. R. (2003). Fracture behavior of hybrid glass matrix composites: thermal ageing effects. *Journal of Composites, Part A: Applied Science and Manufacturing*, 34.
14. Ding, X. D., Jiang, Z. H., Sun, J., Lian, J. S. & Xiao, L. (2002). Stress-strain behavior in initial yield stage of short fiber reinforced metal matrix composite. *Journal of Composites Science and Technology*, 62.
15. Fu, S. Y., Lauke, B., Mäder, E., Yue, C. Y. & Hu, X. (2000). Tensile properties of short-glass-fiber and short-carbon-fiber reinforced polypropylene composites. *Journal of Composites, Part A: Applied Science and Manufacturing*, 31.
16. Koss, D. A., Petrich R. R., Kallas, M. N. & Hellmann, J. R. (1994). Interfacial shear and matrix plasticity during fiber push-out in a metal-matrix composite. *Composites Science and Technology*, 51(1), p. 27.
17. Miserez, A., Rossoll, A. & Mortensen, A. (2004). Investigation of crack-tip plasticity in high volume fraction particulate metal matrix composites. *Engineering Fracture Mechanics*, In Press.
18. Entchev, P. B. & Lagoudas, D. C. (2003). Modeling of transformation-induced plasticity and its effect on the behavior of porous shape memory alloys. *Part II: porous SMA response, Mechanics of Materials*.
19. Lubin, G. (1982). *Handbook of Composite Materials*. Van Nostrand Reinhold Company.
20. Shishehsaz, M. (1995). The effect of oblique cracks on stress distribution in a hybrid composite lamina of finite width. *The 3rd Annual Conference of ISME*, Tehran, Iran.
21. Fukuda, H. & Chou, T. W. (1983). Stress concentration in a hybrid composite sheet. *J. of Applied Mechanics*, 50, 845-848.